

Supplemental File to Ms “Mechanisms of Laser-Induced Dissection and Transport of Histologic Specimens” by A. Vogel et al.

Determination of optical and thermal material properties relevant for laser-induced separation of histologic material

The transmission at $\lambda = 337$ nm of histologic material stained with hematoxylin and eosin (H&E) and of the polymer foil mounted below the histologic sections were measured in the microbeam setup using an energy detector with 1 nJ sensitivity (PD10, Ophir Optronics, Jerusalem, Israel), and in a spectral photometer (Lambda 14 P, Perkin Elmer GmbH, Wellesley, MA, USA). All measurements were performed at low irradiance where nonlinear absorption is negligible. As a reference for unstained biologic material, we also measured the optical properties of a single, confluent layer of cultured cells (Chinese hamster ovary (CHO) cells). The determination of the optical properties of the PEN foil required measurements with an integrating sphere, since PEN scatters strongly at $\lambda = 337$ nm. We measured total transmission and reflection as described in Ref. (1), and calculated the absorption coefficient μ_a and reduced scattering coefficient μ_s' using the Kubelka Munk theory (2,3). The effective attenuation coefficient μ_{eff} and optical penetration depth δ were then obtained by means of the relation (4)

$$\delta = 1/\mu_{eff} = 1/[3\mu_a(\mu_a + \mu_s')]^{1/2}. \quad (1)$$

The heat capacity of the PEN foil and the histologic specimens were determined by differential scanning calorimetry (DSC) in comparison with a sapphire standard (DSC 2920, TA Instruments, New Castle, DE, U.S.A.), and the dissociation temperatures were obtained through thermo-gravimetric analysis (TGA), i.e. by measuring the weight loss as a function of temperature (TGA 2950, TA Instruments, New Castle, DE, U.S.A.).

Time-resolved photography of the laser-induced transport process

The mechanisms of catapulting of histologic specimens were analyzed by time-resolved photography in side view, as shown schematically in Fig. 1. We achieved a temporal resolution better than 20 ns by using single frame photography with increasing time delay between catapulting laser pulse and the instant at which the photograph was exposed. The laser pulses for dissection and catapulting were focused through microscope objective L_0 and a glass slide (GS) onto the specimen of interest. The catapulted specimen was imaged in trans-illumination using the light of a plasma discharge lamp with 18 ns duration (Nanolite KL-L, High-Speed Photo-Systeme, D-22880 Wedel, Germany). We used Koehler-type illumination optics consisting of a $f = 50$ mm, $F = 1.2$ collimator (L_1) and a $f = 250$ mm, $F = 6.2$ condensor (L_2). The long focal length of the condensor provided the large working distance required because of the large width of the microscope stage. The specimens were imaged using a 10x objective (L_3) with a numerical aperture $NA = 0.28$ and 33.5 mm working distance (M Plan Apo, Mitutoyo Corporation, Kawasaki, Japan), and a tube lense (L_4) with 200 mm focal length. In spite of the long working distance of L_3 , a part of the microscope stage had to be milled out to allow for a confocal adjustment of L_3 and L_0 . The intermediate image formed by L_3 and L_4 was further enlarged by a factor of 4.4 using a $f = 105$ mm, $F = 2.8$ macro objective (L_5). Thus the total magnification of the imaging system was 44x, and the spatial resolution (determined by the NA of the long-distance microscope objective) was 2 μm . The relatively large numerical aperture of the imaging system made it sensitive for the detection of plasma luminescence

upon dissection or catapulting. The images were detected using a 6-Megapixel digital camera (FinePix S1 Pro, Fujifilm, Sendai, Japan). Appropriate trigger and delay electronics enabled us to adjust the time between catapulting laser pulse and flash lamp discharge with a precision of a few nanoseconds.

The laser-produced pressure waves, which are phase objects, were visualized by means of a sensitive dark-field Schlieren technique (5). For this purpose, the flash lamp was replaced by a frequency-doubled neodymium:yttrium aluminum garnet (Nd:YAG) laser beam coupled into a 300 m long multimode fiber to destroy temporal coherence. The fiber end served as speckle-free light source for photography with 16 ns exposure time. A vertically oriented thin wire with 50 μm diameter was inserted into the back focal plane of L_5 , and the width of the vertical slit between L_1 and L_2 was adjusted such that the wire exactly blocked the image of the slit. This way, only light deflected by the specimen or the laser-produced pressure waves can reach the digital camera. The Schlieren system is sensitive for the detection of phase gradients in horizontal direction. High sensitivity requires a small size of filter and light source. The slitlike light source makes better use of the available light than what is possible with a dotlike Schlieren filter, which requires a point source. The filter had to be placed in the back focal plane of L_5 because the back focal plane of the microscope objective L_3 is located inside the objective housing and thus not accessible. Waveguide effects in the glass slide GS leading to disturbing background noise were avoided by blackening the edge of the slide facing the illuminating light source. To further reduce the background noise and enhance the visibility of the pressure wave, a reference image was taken at time $t < 0$ and subtracted from each image recorded after the release of the catapulting laser pulse. The initial phase of the catapulting process was documented with time increments of 2 – 60 ns. The high time-resolution allowed to deduce the laser-produced pressure from the speed of the pressure waves (6,7).

It is time consuming to determine the initial values of the specimen's velocity by taking series of images at different time delays. Therefore, we took images with 7 \times magnification at only one delay time (50 μs after the laser pulse) and determined the average velocity during this time in order to investigate parameter dependencies of the flight velocity covering a large parameter range.

References

1. Vogel, A., C. Dlugos, R. Nuffer, and R. Birngruber. 1991. Optical properties of human sclera, and their consequences for transscleral laser applications. *Lasers Surg. Med.* 11:331-340.
2. Cheong, W. F., S. A. Prahl, and A. J. Welch. 1990. A review of the optical properties of biological tissue. *IEEE. J. Quantum Electron.* 26:2166-2185.
3. Star, W. M., J. P. A. Marijnissen, and M. J. C. van Gemert. 1988. Light dosimetry in optical phantoms and in tissues. *Phys. Med. Biol.* 33:437-454.
4. Jacques, S. L. 1993. Role of tissue optics and pulse duration on tissue effects during high-power laser irradiation. *Appl. Opt.* 32:2447-2454.
5. Vogel, A., I. Apitz, S. Freidank, and R. Dijkink. 2006. Sensitive high-resolution white-light Schlieren technique with large dynamic range for the investigation of ablation dynamics. *Opt. Lett.* 31:1812-1814.
6. Vogel, A., S. Busch, and U. Parlitz, U. 1996. Shock wave emission and cavitation bubble generation by picosecond and nanosecond optical breakdown in water. *J. Acoust. Soc. Am.* 100:148-165.
7. Apitz, I., and A. Vogel. 2005. Material ejection in nanosecond Er:YAG laser ablation of water, liver, and skin. *Appl. Phys. A* 81:329-338.

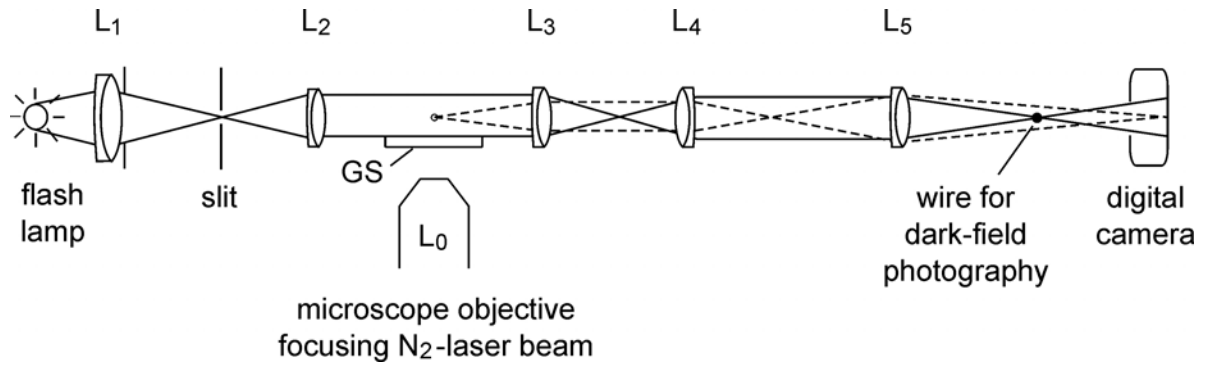


Fig. 1 Setup for time-resolved photography of the dynamics of transport processes in a laser-microbeam apparatus.